RESEARCH ARTICLE | AUGUST 19 2021

Collision rates of permeable particles in creeping flows *⊗*

Rodrigo B. Reboucas [0]; Michael Loewenberg [20]



Physics of Fluids 33, 083322 (2021) https://doi.org/10.1063/5.0060018





Articles You May Be Interested In

On the hydrodynamic interaction between a particle and a permeable surface

Physics of Fluids (July 2013)

The singular hydrodynamic interactions between two spheres in Stokes flow

Physics of Fluids (June 2020)

A slender-body theory for low-viscosity drops in shear flow between parallel walls

Physics of Fluids (April 2010)



Physics of Fluids

Special Topics Open for Submissions

Learn More



Collision rates of permeable particles in creeping flows

Cite as: Phys. Fluids 33, 083322 (2021); doi: 10.1063/5.0060018

Submitted: 15 June 2021 · Accepted: 26 July 2021 · Published Online: 19 August 2021







Rodrigo B. Reboucas (in and Michael Loewenbergal) (in



AFFILIATIONS

Department of Chemical and Environmental Engineering, Yale University, New Haven, Connecticut 06520-8286, USA

a) Author to whom correspondence should be addressed: michael.loewenberg@yale.edu

ABSTRACT

Binary collision rates are calculated for the permeable particles undergoing (i) Brownian motion, (ii) gravity sedimentation, (iii) uniaxial straining flow, and (iv) shear flow. Darcy's law is used to describe the flow inside the permeable particles, and no-slip boundary conditions are applied at particle surfaces. A leading-order asymptotic solution of the problem is developed for the weak permeability regime $K = k/a^2 \ll 1$, where $k = \frac{1}{2}(k_1 + k_2)$ is the mean permeability and $a = a_1 a_2/(a_1 + a_2)$ is the reduced radius; a_i , k_i (i = 1, 2), respectively, is the radius and permeability of each particle. The resulting collision rates are given by the quadrature of the pair mobility functions for permeable particles in the near-contact lubrication region and size-ratio-dependent parameters obtained from standard hard-sphere pair mobility functions. Collision rates in shear flow vanish below a critical value of the permeability parameter K* that increases with diminishing size ratio. The analogous problem of pair collision rates of particles with small-amplitude surface roughness δa is also analyzed. The formulas for the collision rates of rough particles provide accurate analytical approximations for the collision rates of permeable particles for all four aggregation mechanisms and a wide range of size ratios using an equivalent roughness $\delta=0.72K^{2/5}$.

Published under an exclusive license by AIP Publishing. https://doi.org/10.1063/5.0060018

I. INTRODUCTION

The aggregation of particles suspended in fluids has been the subject of intense theoretical and practical investigations for over a century. Examples of applications encompass deep-bed granular filtration, rain-drop formation, and particle coagulation in marine environments, e.g., marine "snow." A fundamental description of the rates of particle encounters is crucial in properly characterizing the resulting suspension stability and microstructure.

The rate of coagulation in a dilute dispersion of impermeable particles was first investigated by Smoluchoswski in 1917 who proposed a model for analyzing interparticle encounters, neglecting the hydrodynamic interactions and assuming a sticking force at contact. Fuchs⁸ proposed a correction to Smoluchowski's model for electrically charged aerosol particles. Spielman,9 Valioulis and List,10 and Kim and Zukoski¹¹ analyzed the perikinetic (Brownian) coagulation of spherical colloidal particles, accounting for pairwise hydrodynamic interactions and non-hydrodynamic interparticle forces, such as the van der Waals attraction and electrostatic repulsion.

Curtis and Hocking, 12 Arp and Mason, 13 Zeichner and Schowalter,¹⁴ Van de Ven and Mason,¹⁵ and Adler¹⁶ studied the orthokinetic coagulation: particle coagulation in suspensions undergoing prescribed flows, including shear flow, and uniaxial straining flow.

Particle coagulation in more general flows has also been considered. 17-19 In these studies, the pairwise hydrodynamic interactions and non-hydrodynamic interparticle forces²⁰ were incorporated in a trajectory analysis.^{21–25} Coagulation of sedimenting particles has also been analyzed using trajectory calculations that incorporate the hydrodynamic interactions and interparticle forces.^{26–2}

The foregoing analyses only consider the pairwise particle interactions; thus, their application is limited to semi-dilute suspensions. Pairwise coagulation rates are usually expressed in a dimensionless form as a collision efficiency, E, i.e., the rate of coagulation normalized by the coagulation rate in the absence of hydrodynamic and nonhydrodynamic forces (i.e., as predicted by Smoluchowski's theory⁷) stability ratio is defined as the reciprocal of the collision efficiency, E^{-1} .

Davis and co-workers investigated the effects of hydrodynamic interactions and interparticle forces on the collision efficiency of spherical drops in Brownian motion, sedimentation, ³⁰ linear flows, ³ and particle flotation by bubbles or drops.³³ These studies show that interfacial mobility significantly enhances the collision efficiency of drops compared to the no-slip boundary conditions appropriate for

The analysis in most of the foregoing studies is restricted to either the small- or large-Peclet number limit. Exceptions include

Zinchencko and Davis³⁴ and Bal^{35,36} who investigated the coagulation rates in colloidal suspensions by the combination of Brownian motion and shear flow at arbitrary Peclet numbers, and Zinchenko and Davis³⁷ and Ramirez *et al.*³⁸ who evaluated coagulation rates by the combination of Brownian motion and sedimentation at arbitrary Peclet number.

Due to the classical lubrication singularity for vanishing surface-to-surface separations, $h_0 \rightarrow 0$ (i.e., contact), collisions between smooth spherical (impermeable) particles are possible only in the presence of material-specific non-hydrodynamic attractive forces (e.g., van der Waals forces), or generic physical phenomena, including surface roughness or particle permeability³⁹ that lead to a breakdown of the lubrication singularity at contact.

Particles with surface roughness amplitude δa are usually treated as smooth spherical particles, where the surface-to-surface separation is restricted according to $h_0 \geq \delta a$, contact occurs at $h_0 = \delta a$, and the roughness amplitude is assumed to be small compared to the particle size, $\delta \ll 1$. Two limits for the coefficient of contact friction have been considered: zero and infinite, corresponding to perfect slip and noslip, respectively, but the results are insensitive to this choice ^{43,44} because the viscous transverse lubrication resistance acting over the near-contact region dominates the friction acting at the point of contact.

The investigation of the collision efficiency of permeable particles dates back to 1967 when Sutherland⁴⁵ proposed a geometric model for the formation of high-porosity aggregates based on Smoluchowski's diffusion equation. Following this previous work, a significant body of research has been focused on the aggregate formation and collision rates of particle aggregates (flocs) with highly porous structure. Often, Brinkman's equation⁴⁶ is used for describing the flow inside highly porous aggregates. 47-50 Neale et al. 51 proposed a correction factor to the Stokes drag on a settling permeable sphere to account for the permeable effects and examined the assumption that an isolated highporosity aggregate may be modeled as an impermeable body.⁵ Adler⁵³ analyzed the streamlines using Brinkman's equation for the flow inside permeable spheres to predict aggregation-disaggregation dynamics. Further theoretical and experimental works on the aggregation kinetics of fractal aggregates with radially varying permeability showed that collision efficiencies decreased with the fractal dimension while the viscous drag increased.5

Bäbler *et al.*⁵⁸ used the method of reflections⁵⁹ to study the pairwise hydrodynamic interactions of high-porosity aggregates in linear flows using Brinkman's equation to describe flow inside the aggregate. Collision efficiencies were estimated from a trajectory analysis with and without the van der Waals forces. The same author used the foregoing trajectory analysis scheme to explore the collision efficiency of aggregates accounting for fractal dimension, internal structure, and interparticle forces. Near-field and lubrication interactions were unresolved in these studies, and perhaps justified, by the restriction to particles with high porosities.

Problems involving thin permeable layers or membranes have been extensively studied, 61–66 including the collision efficiency for particles captured by drops with a permeable interface. 67 In these problems, the thin permeable layer reduces to a normal velocity boundary condition. Core–shell particles comprised of a comparatively thin, highly porous shell and impermeable core have been analyzed using Brinkman's equation to describe the fluid flow in the shell, 68,69 and collision efficiencies have been calculated. 70

Darcy's law⁷¹ is usually a more appropriate model than Brinkman's equation for describing flow in porous particles. Slipvelocity boundary conditions apply $^{72-74}$ but no-slip boundary conditions are often used. Brinkman's equation was derived for creeping flow through dilute, fixed arrays of particles. $^{46,75-77}$ Despite its wide use for flow in porous materials, Brinkman's equation is only valid for very high porosities, and even then, only for specific microstructures, 78 e.g., arrays of spheres with $\geq 95\%$ porosity. Often, it happens that the Brinkman term (Laplacian of the velocity), while physically unjustified, has a negligible effect so that the Brinkman equation reduces to Darcy's law.

Reboucas and Loewenberg^{39,80} developed a lubrication analysis for permeable spheres in close contact, $h_0/a \ll 1$, under the weak permeability conditions,

$$K = k/a^2 \ll 1. \tag{1.1}$$

Here, h_0 is the surface-to-surface separation, $a = a_1 a_2 (a_1 + a_2)^{-1}$ is the reduced radius, k is the mean permeability of the particles,

$$k = \frac{1}{2}(k_1 + k_2), \qquad (1.2)$$

and K is the dimensionless permeability. Their analysis showed that axisymmetric mobilities for weakly permeable particles are qualitatively affected for gap widths $h_0/a = O(K^{2/5})$, and, in contrast to the impermeable spheres, have non-zero $O(K^{2/5})$ values at contact. Accordingly, the particle contact is predicted to occur in finite time under the action of a constant force, leading to finite collision efficiencies even in the absence of non-hydrodynamic forces or surface roughness. This is partially offset by the discovery that permeability causes particles to spend less time in close contact because the transverse hydrodynamic interactions are also reduced. 80

The weak permeability limit, $K \to 0$, is singular. The particle permeability affects the trajectories at O(1) within a thin $O(K^{2/5})$ boundary layer that forms in the near-contact region outside of the contact surface. Away from the boundary layer, $h_0/a \gg K^{2/5}$, permeability has a weak O(K) effect. Surface roughness is an analogous physical phenomenon that circumvents the lubrication singularity and forms a δ -thickness boundary layer. These situations are similar to the $O(A_H/\mu a^2 U_{12}^\infty)^{1/2}$ thickness boundary layer that forms in the near-contact region for the impermeable particles in limit of the weak van der Waals forces, $A_H \to 0$, where A_H is the Hamaker constant, U_{12}^∞ is the relative velocity of the particles at large separations, a is the particle size, and μ is the fluid viscosity.

In this paper, the collision efficiency of permeable particles is analyzed for aggregation in Brownian motion, gravity sedimentation, uniaxial straining flow, and shear flow, each separately considered. Weak permeability conditions (1.1) are assumed. As an example, permeabilities for partially sintered ceramics are $O(10^{-18})$ m², 82,83 corresponding to $K=10^{-8}$ for 10 μ m particles. Darcy's law is used to describe the intraparticle flow, and no-slip boundary conditions are applied at the particle surfaces. Collision efficiencies are derived for spheres with small-amplitude surface roughness and the two problems are shown to be analogous through the definition of an equivalent roughness for permeable particles. The resulting formulas provide accurate closed-form analytical approximations for the collision efficiencies of permeable spheres. The focus here is on the physical mechanism of particle permeability; thus, the van der Waals attraction is included only for

collision efficiencies in Brownian motion and neglected in calculations of collision efficiencies in flow and sedimentation under the assumption of large Peclet numbers, as explained below. The problem is formulated in Sec. II, and the assumptions are discussed. Collision efficiency formulas are derived for permeable particles in Sec. III and for rough particles in Sec. IV. The results are graphically presented and discussed in Sec. V. Concluding remarks are made in Sec. VI.

II. PROBLEM FORMULATION

In a dilute suspension, the pair-distribution function, p_{12} , is governed by the steady-state Fokker-Plank equation,

$$\nabla \cdot (p_{12}V_{12}) = 0, \qquad (2.1)$$

where V_{12} is the relative velocity of the particles. Particles are assumed to aggregate on contact; thus, $p_{12} = 0$ on a spherical contact surface with radius $r = a_1 + a_2$, where a_1 and a_2 are the particle radii; far from the contact surface, $p_{12} = 1$.

The relative velocity of the particles is given by 22,24

$$\mathbf{V}_{12} = -D_{12}^{(0)}[G(s)\hat{\mathbf{r}}\hat{\mathbf{r}} + H(s)(\mathbf{I} - \hat{\mathbf{r}}\hat{\mathbf{r}})] \cdot \mathbf{V} \left(\log p_{12}(\mathbf{r}) + \frac{\Phi_{12}(s)}{k_B T}\right) + [L(s)\hat{\mathbf{r}}\hat{\mathbf{r}} + M(s)(\mathbf{I} - \hat{\mathbf{r}}\hat{\mathbf{r}})] \cdot \mathbf{V}_{12,g}^{(0)} + \mathbf{E}_{\infty} \cdot \mathbf{r} + \boldsymbol{\omega}_{\infty} \times \mathbf{r} - [A(s)\hat{\mathbf{r}}\hat{\mathbf{r}} + B(s)(\mathbf{I} - \hat{\mathbf{r}}\hat{\mathbf{r}})] \cdot \mathbf{E}_{\infty} \cdot \mathbf{r}.$$
(2.2)

Here, $\mathbf{r} = \mathbf{r}_2 - \mathbf{r}_1$ is the vector between the particle centers, $\hat{\mathbf{r}} = \mathbf{r}/|\mathbf{r}|$ is a unit vector along the line-of-centers, I is the identity tensor, and $s = |\mathbf{r}|/\bar{a}$ is the center-to-center separation normalized by the average radius (2.8). The quantities \mathbf{E}_{∞} and $\boldsymbol{\omega}_{\infty}$ are the imposed rate-of-strain and vorticity in the fluid. The quantities k_B and T are Boltzmann's constant and absolute temperature; Φ_{12} is the interparticle potential. The quantities $D_{12}^{(0)}$ and $\mathbf{V}_{12,g}^{(0)}$ are, respectively, the Stokes–Einstein– Sutherland relative diffusivity and gravitational particle velocities in the absence of hydrodynamic interactions (i.e., $s \to \infty$),

$$D_{12}^{(0)} = k_B T \left(m_1^{(0)} + m_2^{(0)} \right), \quad \mathbf{V}_{12,g}^{(0)} = |\mathbf{F}_{1,g} m_1^{(0)} - \mathbf{F}_{2,g} m_2^{(0)}|, \quad (2.3)$$

where

$$m_i^{(0)} = \frac{1 + K_i}{6\pi \mu a_i}$$
 (i = 1,2), (2.4)

are the hydrodynamic mobilities of isolated permeable particles in Stokes flow with no-slip boundary conditions, and

$$\mathbf{F}_{i,g} = \frac{4\pi}{3} a_i^3 \Delta \rho \, \mathbf{g} \quad (i = 1, 2),$$
 (2.5)

are the net gravity forces acting on the particles. Here, k_i are the particle permeabilities and $K_i = k_i/a_i^2$ are the dimensionless permeabilities, μ is the fluid viscosity, ${f g}$ is the acceleration of gravity, and $\Delta
ho =
ho_{
ho} -
ho_0$ is the excess particle density, where ρ_0 and ρ_p are, respectively, the density of the suspending fluid and the particles (assumed the same for both).

Equation (2.2) defines the pairwise axisymmetric and transverse mobility functions G, L, A and H, M, B, respectively. According to their definitions, G, H, L, and M tend to unity at large separations, whereas *A* and *B* vanish for $s \to \infty$. The pair mobilities depend on the center-to-center separation s, particle permeabilities K_i (i = 1, 2), and size ratio $\kappa = a_2/a_1$. The linear superposition inherent in the form of the relative particle velocity (2.2) is predicated on the assumption of small Reynolds numbers,

$$Re = \frac{\rho V_{12}^{(0)} a}{u} \ll 1, \qquad (2.6)$$

where $V_{12}^{(0)}=|\mathbf{V}_{12}^{(0)}|$, and ρ is the fluid density. For the weak permeability regime $K\ll 1$ considered herein, the particle mobilities are affected by the permeability only in the nearcontact region and only by the mean permeability (1.2). Outside of this region, the particle mobilities are approximately equal to the mobilities of impermeable particles. Impermeable particles with smallamplitude surface roughness, $\delta \ll 1$, will also be analyzed because of the useful analogy it provides. In this case, impermeable mobility functions apply everywhere away from the contact surface at $r = a_1 + a_2$ $+\delta a$, where a is the reduced radius (2.9). For either of these cases, isolated mobilities for impermeable spheres, $(6\pi\mu a_i)^{-1}(i=1,2)$, can be used in place of the isolated mobilities for permeable spheres (2.4). Accordingly, (2.3) simplifies to

$$D_{12}^{(0)} = \frac{k_B T}{6\pi \mu a} , \quad \mathbf{V}_{12,g}^{(0)} = \frac{2(a_1^2 - a_2^2)\Delta\rho \,\mathbf{g}}{9\mu} . \tag{2.7}$$

Different length normalizations are convenient in different contexts. For convenience, these are summarized here. The average and reduced radius are defined,

$$\bar{a} = \frac{1}{2}(a_1 + a_2) = \frac{1}{2}a_1(1+\kappa),$$
 (2.8)

$$a = a_1 a_2 (a_1 + a_2)^{-1} = a_1 \kappa (1 + \kappa)^{-1} = \nu \bar{a}$$
, (2.9)

where $\kappa = a_2/a_1$ denotes the size ratio and ν is the conversion factor between the average and reduced radius which arises in the analysis to

$$\nu = \frac{a}{\bar{a}} = 2\kappa (1 + \kappa)^{-2} \,. \tag{2.10}$$

The center-to-center separation r and surface-to-surface separation h_0 are both relevant, and two corresponding dimensionless lengths are used,

$$s = \frac{r}{\bar{a}} \tag{2.11}$$

and

$$\epsilon = \frac{h_0}{a}; \quad \xi = s - 2 = \frac{h_0}{\bar{a}} = \nu \epsilon. \tag{2.12}$$

A. van der Waals attraction

Herein, consideration of interparticle forces is limited to the unretarded van der Waals potential,

$$\Phi_{12} = A_H \bar{\Phi}_{12} \,, \tag{2.13}$$

where A_H is the Hamaker constant, and $\bar{\Phi}_{12}$ is the dimensionless

$$\bar{\Phi}_{12}(s) = -\frac{1}{6} \left(\frac{8\kappa}{(\kappa+1)^2 (s^2 - 4)} + \frac{8\kappa}{(\kappa+1)^2 s^2 - 4(1-\kappa)^2} + \log \left[\frac{(\kappa+1)^2 (s^2 - 4)}{(\kappa+1)^2 s^2 - 4(1-\kappa)} \right] \right), \tag{2.14}$$

which has the singular form at contact,

$$\bar{\Phi}_{12}(\xi) = -\frac{\nu}{6\xi} + O(\log \xi) \,, \quad \xi \ll 1 \,, \tag{2.15}$$

where κ , ξ , and ν are defined above.

The dimensionless Hamaker parameter,

$$\bar{A}_H = A_H / k_B T, \tag{2.16}$$

characterizes the relative strength of the van der Waals attraction in Brownian motion; typically, $\bar{A}_H = O(1)$. The relative strength of the van der Waals interactions for non-diffusing particles, aggregating under gravity-driven sedimentation or in a prescribed flow, is characterized by the parameter Q_H which is related to the Peclet number,

$$Q_H = \frac{Pe}{\bar{A}_H}, \quad \text{Pe} = \frac{\mu V_{12}^{(0)} a^2}{k_B T},$$
 (2.17)

where $V_{12}^{(0)}$ is given by (2.7) for sedimentation and $V_{12}^{(0)}=E_{\infty}a$ for particles in flow, where E_{∞} is the imposed strain rate. Often, $\text{Pe}\gg 1$ and thus $Q_H\gg 1$. Consider, for example, 30 μm particles in a fluid with viscosity $\mu=.01$ Pa s and $\bar{A}\approx 1$ for two situations: (i) sedimenting in normal gravity with $\Delta\rho/\rho=2$ and (ii) in shear flow with shear-rate $E_{\infty}=10~\text{s}^{-1}$. For both of these cases, $Q_H\approx 10^6$ [and Re $\approx.001$, where the Reynolds number is defined by Eq. (2.6)].

Even for $Q_H\gg 1$, the van der Waals attraction can be important because of its singular behavior (2.15). Balancing the $O(\mu V_{12}^{(0)}a)$ viscous and $O(A_Hah_0^{-2})$ van der Waals forces acting on the particles in close contact yields the $O(A_H/\mu a^2 U_{12}^\infty)^{1/2}$ boundary layer associated with the weak van der Waals attraction. ^{27,81} Comparing to the $O(K^{2/5})$ boundary layer associated with the particle permeability indicates that van der Waals attraction is negligible if

$$K \gg Q_H^{-5/4}$$
 (2.18)

The van der Waals attraction is included in our analysis of aggregation in Brownian motion because $\bar{A}_H = O(1)$ is typical. However, the van der Waals attraction is omitted in our collision efficiency calculations for non-diffusing particles aggregating under sedimentation or in an imposed flow under the assumption that Eq. (2.18) holds. Herein, the focus is on permeability and surface roughness as physical mechanisms that give rise to non-zero collision rates in the absence of non-hydrodynamic forces. The complementary regime of particle collisions mediated by colloidal forces has been the subject of numerous classical investigations, such as those discussed in the Introduction.

B. Collision efficiencies

In this section, pairwise aggregation rates are defined and the classical formulas for collision efficiencies, given in terms of pair mobility functions, are recalled for particles in Brownian motion, gravity sedimentation, and in imposed uniaxial straining and shear flows; each case is separately considered.

The pairwise aggregation rate of particles J_x is given by the integral of the flux over the contact surface at $r = r_o^{27}$

$$J_x = -n_1 n_2 \int_{r_*} p_{12} V_{12} \cdot \boldsymbol{n} \, dS, \qquad (2.19)$$

where $r_c = a_1 + a_2 + \delta a$ for particles with surface roughness, otherwise $r_c = a_1 + a_2$. Here, n_i (i = 1, 2) are the upstream number densities of the particles, and subscript x = B, g, st, sh, respectively, will be used to denote aggregation in Brownian motion, gravity sedimentation, straining flow, and shear flow. Collision efficiencies are defined as

$$E_x = J_x / J_x^{(0)} \,, \tag{2.20}$$

where $J_x^{(0)}$ is the aggregation rate in the absence of hydrodynamic interactions (i.e., G = H = L = M = 1 and A = B = 0). Collision rates under these conditions are given by

$$J_B^{(0)} = 4\pi n_1 n_2 D_{12}^{(0)} (a_1 + a_2), \tag{2.21a}$$

$$J_{\sigma}^{(0)} = n_1 n_2 V_{12,\sigma}^{(0)} \pi (a_1 + a_2)^2, \tag{2.21b}$$

for aggregation in Brownian motion and gravity sedimentation, and

$$J_{st}^{(0)} = \frac{8\pi}{3\sqrt{3}} n_1 n_2 E_{\infty} (a_1 + a_2)^3, \qquad (2.22a)$$

$$J_{sh}^{(0)} = \frac{4}{3} n_1 n_2 E_{\infty} (a_1 + a_2)^3, \qquad (2.22b)$$

for aggregation in uniaxial straining flow and shear flow. Here, $D_{12}^{(0)}$ and $V_{12,g}^{(0)}$ are given by Eq. (2.7), and E_{∞} is the imposed strain rate.

Collision efficiencies are obtained for each aggregation mechanism, by appropriately simplifying the relative particle velocity (2.2), inserting it into Eq. (2.1), and integrating with boundary conditions,

$$p_{12}(s_c) = 0$$
 and $p_{12}(\infty) = 1$, (2.23)

where $s_c = r_c/\bar{a}$.

The collision efficiency for Brownian motion is obtained by simplifying Eq. (2.2) for neutrally buoyant particles in a quiescent fluid [i.e., $V_{12,g}^{(0)} = \mathbf{E}_{\infty} = \boldsymbol{\omega}_{\infty} = 0$]. Integrating the resulting radial velocity in Eq. (2.1) and applying boundary conditions (2.23) yield

$$E_B = 1/I_B(s_c),$$
 (2.24a)

$$I_B(s) = 2 \int_s^\infty \frac{e^{\bar{A}_H \bar{\Phi}(s)}}{s^2 G(s)} ds$$
. (2.24b)

As indicated, the van der Waals attraction is retained in the above formula for the binary collision efficiency of particles in Brownian motion. The formulas below for collision efficiencies in sedimentation and linear flows are derived with the van der Waals attraction omitted, as discussed in Sec. II A.

The collision efficiency for gravity sedimentation is obtained by inserting Eq. (2.2) simplified for non-diffusing particles in a quiescent fluid [i.e., $D_{12}^{(0)} = \mathbf{E}_{\infty} = \omega_{\infty} = 0$] into Eq. (2.1). Dividing the resulting components of the relative velocity normal, and parallel, to the line-of-centers, and integrating the critical trajectory upstream from the equator of the contact surface to determine the radius of the upstream collision cross section, yield^{24,27}

$$E_g = e^{2I_g(s_c)}, (2.25a)$$

$$I_g(s) = \int_s^\infty \frac{L(s) - M(s)}{L(s)} \frac{ds}{s}.$$
 (2.25b)

The collision efficiency for uniaxial straining flow is similarly obtained after inserting Eq. (2.2), simplified for non-diffusing, neutrally buoyant

particles in an axisymmetric flow [i.e., $D_{12}^{(0)}=V_{12,g}^{(0)}=\omega_\infty=0$], into Eq. (2.1). The result is ^{22,23,31}

$$E_{st} = e^{-3I_{st}(s_c)}, (2.26a)$$

$$I_{st}(s) = \int_{s}^{\infty} \frac{A(s) - B(s)}{1 - A(s)} \frac{ds}{s}.$$
 (2.26b)

A more complicated picture arises in shear flow due to the existence of nearby recirculating (closed) particle trajectories that do not contribute to particle aggregation at steady state and must be subtracted from the net particle flux on the contact surface. The collision efficiency in this case is given by³¹

$$E_{sh} = \left(e^{-2I_{st}(s_c)} - I_{sh}(s_c)\right)^{3/2}, \tag{2.27a}$$

$$I_{sh}(s) = \frac{1}{4} \int_{s}^{\infty} e^{-2I_{st}} \frac{B(s)}{1 - A(s)} s ds,$$
 (2.27b)

where $e^{-2I_{st}}-I_{sh}>0$ is assumed; for $e^{-2I_{st}}-I_{sh}\leq 0$, $E_{sh}\equiv 0$.

C. Permeable particles

For permeable particles, the pairwise mobilities that appear in Eq. (2.2) depend on the particle separation, the size ratio, and the permeability parameter q_s^{39}

$$q = \epsilon K^{-2/5} = \nu^{-1} \xi K^{-2/5}$$
, (2.28)

where K is the dimensionless mean permeability and ϵ is the dimensionless gap (2.12).

Under the weak permeability conditions (1.1), the particle mobilities are approximately the same as those for impermeable particles with O(K) error for $q \gg 1$, but they are qualitatively altered for q = O(1). The near-contact axisymmetric mobilities for permeable particles exhibit a simplified, separable dependence on permeability, ⁸⁰

$$G_{\xi} = \nu^{-1} \frac{\xi}{f(q)},$$
 (2.29a)

$$L_{\xi} = R_g(\kappa) \frac{\xi}{f(q)},\tag{2.29b}$$

$$A_{\xi} = 1 - R_{st}(\kappa) \frac{\xi}{f(q)}, \qquad (2.29c)$$

where R_g and R_{st} , respectively, are the dimensionless contact resistances that arise for particles in point-contact migrating parallel to their line-of-centers in gravity and uniaxial straining flow. The function f(q) is the numerical solution of an axisymmetric Reynolds lubrication equation³⁹ that has the asymptotic properties,

$$f(q) = c_1 q - c_2 q^2 + O(q^2), \quad q \ll 1,$$
 (2.30a)

$$f(q) = 1 - c_3 q^{-5/2} + O(q^{-5}), \quad q \gg 1,$$
 (2.30b)

where $c_1 \doteq 0.7507$, $c_2 \doteq 0.224$, and $c_3 \doteq 1.8402$. Inserting Eqs. (2.28) and (2.30a) into Eq. (2.29) reveals that the axisymmetric mobilities of permeable particles have non-zero $O(K^{2/5})$ contact values in contrast to the vanishing mobilities at contact for impermeable particles.⁸⁰ This is why the permeable particles can aggregate even in the absence of interparticle forces.

The transverse mobilities *M* and *B* have the lubrication forms

$$M_{\xi} = \frac{m_1 + m_2 \log \xi^{-1} + m_3 \left[\log \xi^{-1} - \frac{5}{12} g(q) \right] \log \xi^{-1} + m_6 g(q)}{m_4 + m_5 \log \xi^{-1} + \left[\log \xi^{-1} - \frac{5}{12} g(q) \right] \log \xi^{-1} + m_7 g(q)},$$
(2.31a)

$$B_{\xi} = \frac{b_1 + b_2 \log \xi^{-1} + b_3 \left[\log \xi^{-1} - \frac{5}{12} g(q) \right] \log \xi^{-1} + b_6 g(q)}{b_4 + b_5 \log \xi^{-1} + \left[\log \xi^{-1} - \frac{5}{12} g(q) \right] \log \xi^{-1} + b_7 g(q)},$$
(2.31b)

where the coefficients m_i and b_i (i = 1–9) depend on the size ratio. The function g(q) is the numerical solution of a transverse Reynolds lubrication equation ⁸⁰ with the asymptotic properties,

$$g(q) = -\frac{12}{5}\log q + c_4 + O(q), \quad q \ll 1,$$
 (2.32a)

$$g(q) = c_5 q^{-5/2} + O(q^{-5}), \quad q \gg 1,$$
 (2.32b)

with $c_4 \doteq -0.48$ and $c_5 \doteq 2.12$. Inserting the limiting result (2.32a) for $q \to 0$ into Eq. (2.31), yields permeability-dependent contact values for the transverse mobilities.⁸⁰

The lubrication forms of the classical mobility functions are

$$G_{\xi,0} = \nu^{-1} \xi \,, \tag{2.33a}$$

$$L_{\xi,0} = R_g(\kappa) \, \xi, \tag{2.33b}$$

$$A_{\xi,0} = 1 - R_{st}(\kappa) \, \xi \tag{2.33c}$$

and

$$M_{\xi,0} = \frac{m_1 + m_2 \log \xi^{-1} + m_3 \log^2 \xi^{-1}}{m_4 + m_5 \log \xi^{-1} + \log^2 \xi^{-1}}, \qquad (2.34a)$$

$$B_{\xi,0} = \frac{b_1 + b_2 \log \xi^{-1} + b_3 \log^2 \xi^{-1}}{b_4 + b_5 \log \xi^{-1} + \log^2 \xi^{-1}}.$$
 (2.34b)

These results are recovered from formulas (2.29) and (2.31) by setting f=1 and g=0, corresponding to $q\to\infty$, according to Eqs. (2.30b) and (2.32b).

Away from the near-contact region, the particle mobilities are approximated by the mobilities of impermeable particles, denoted by G_0, L_0, A_0, M_0, B_0 , under the assumption of weak permeability, as discussed above.

III. COLLISION EFFICIENCY FORMULAS FOR PERMEABLE PARTICLES

In this section, a leading-order asymptotic formulation is presented for the computation of collision efficiencies of weakly permeable particles. Collision efficiencies are determined by the values of the collision efficiency integrals (2.24)–(2.27) on the contact surface at s=2. The formulation employs a uniformly valid approximation of the integrands in Eqs. (2.24b)–(2.27b) for $K\ll 1$. The resulting collision efficiencies are given by a quadrature of lubrication approximations for the mobility functions of permeable particles in the near-contact region, and the size-ratio-dependent parameters are derived from standard hard-sphere mobilities. The details of the generic

derivation are provided in Appendix A, and the procedure for evaluating the formulas is provided in Appendix B.

A. Collision efficiency for Brownian motion

The binary collision efficiency for permeable particles undergoing Brownian motion is given by Eq. (2.24). The collision efficiency integral (2.24b) is evaluated on the contact surface by the procedure described in Appendix A1. Accordingly, the functions P(s) and Q in Eq. (A1) are given by

$$Q(s) = G(s), (3.1a)$$

$$P(s) = \frac{2e^{\bar{A}_H\bar{\Phi}(s)}}{s^2}$$
, (3.1b)

and correspondingly, by Eqs. (2.29a) and (2.15),

$$Q_{\xi} = \frac{\nu^{-1}\xi}{f(q)} \,, \tag{3.2a}$$

$$P_{\xi} = \frac{e^{-\frac{\nu A_H}{6\xi}}}{2} \,. \tag{3.2b}$$

The corresponding function, G_0 , for impermeable spheres is also required, and in the lubrication regime is given by Eq. (2.33a). The required indefinite integral (A11) is

$$F_B(x) = \nu \int_0^x e^{-\frac{\nu A_H}{6\xi}} \frac{d\xi}{2\xi} = \frac{\nu}{2} E_1 \left(\frac{\nu \bar{A}_H}{6x}\right),$$
 (3.3)

where $E_1 = \int_{r}^{\infty} e^{-t} dt/t$ is the exponential integral.

Inserting Eqs. (3.1)–(3.3) into Eq. (A12) and the result into Eq. (2.24) yields the collision efficiency,

$$E_B^{(k)} = \left[\Gamma_B + \Lambda_B^{(0)} - \frac{\nu}{2} E_1(A_k) \right]^{-1},$$
 (3.4)

where

$$\Gamma_{B} = \lim_{\xi \to 0} \left[\int_{\xi}^{\infty} \frac{2e^{\bar{A}_{H}\bar{\Phi}(t)}}{(2+t)^{2}G(t)} dt + \frac{\nu}{2} E_{1} \left(\frac{\nu \bar{A}_{H}}{6\xi} \right) \right]
= \int_{0}^{\infty} \frac{2e^{\bar{A}_{H}\bar{\Phi}(t)}}{(2+t)^{2}G(t)} dt \quad \bar{A}_{H} > 0$$
(3.5)

and

$$\Lambda_B^{(0)} = \frac{\nu}{2} \left[\int_1^\infty e^{-A_k/q} [f(q) - 1] \frac{dq}{q} + \int_0^1 e^{-A_k/q} f(q) \frac{dq}{q} \right]. \tag{3.6}$$

Here, the parameter A_k is the modified Hamaker parameter for permeable particles,

$$A_k = \frac{\bar{A}_H}{6K^{2/5}} \,. \tag{3.7}$$

For $A_k \ll 1$, Eqs. (3.1b), (3.1b), and (3.3) reduce to

$$P(s) = \frac{2}{s^2},\tag{3.8a}$$

$$P_{\xi} = \frac{1}{2},$$
 (3.8b)

and

$$F_{B,0}(x) = \frac{\nu}{2} \log x$$
, (3.9)

yielding the collision efficiency,

$$E_B^{(k)} = \left[\Gamma_{B,0} + \Lambda_{B,0}^{(0)} - \frac{\nu}{2} \log \nu K^{2/5}\right]^{-1}, \quad A_k \ll 1,$$
 (3.10)

where

$$\Gamma_{B,0} = \lim_{\xi \to 0} \left[\int_{\xi}^{\infty} \frac{2}{(2+t)^2 G(t)} dt + \frac{\nu}{2} \log \xi \right]$$
(3.11)

and

$$\Lambda_{B,0}^{(0)} = \frac{\nu}{2} \left[\int_{1}^{\infty} [f(q) - 1] \frac{dq}{q} + \int_{0}^{1} f(q) \frac{dq}{q} \right] \doteq 0.1626 \,\nu. \tag{3.12}$$

Here, $\Gamma_{B,0}$ depends only on the size ratio, and $\nu^{-1}\Lambda_{B,0}^{(0)}$ has the indicated constant value. The numerical value of this integral was previously computed to determine the contact time between the permeable particles under the action of a constant force [Ref. 39, Eq. (4.24)].

The effect of the particle permeability vanishes in the complementary limit of the strong van der Waals attraction, $\bar{A}_k \gg 1$, and the classical result $E_B^{(0)}$ for impermeable spheres is recovered,

$$E_B^{(0)} = \Gamma_B^{-1} \,, \tag{3.13}$$

with Γ_B given by Eq. (3.5).

B. Collision efficiency for sedimentation

The collision efficiency for permeable particles undergoing sedimentation is given by Eq. (2.25). The collision efficiency integral (2.25b) is evaluated on the contact surface by the procedure in Appendix A1. The required functions in Eq. (A1) are thus

$$Q(s) = L(s), \quad P(s) = (L(s) - M(s))s^{-1},$$
 (3.14)

and from Eqs. (2.29b) and (2.31a), the lubrication forms are

$$Q_{\xi} = R_g \frac{\xi}{f(q)}, \quad P_{\xi} = -\frac{1}{2} M_{\xi}(\xi, q).$$
 (3.15)

The corresponding functions, L_0 and M_0 , for impermeable spheres are also required; their lubrication forms are given by Eqs. (2.33b) and (2.34a). Here, the required indefinite integral (A11) is

$$F_g(x) = -\frac{1}{R_*} \int_{-\infty}^{x} M_{\xi,0}(t) \frac{dt}{2t} = \log f_g(x),$$
 (3.16)

and $f_g(x)$ is given by Eq. (A30) in Appendix A4. Inserting this result with Eqs. (3.14) and (3.15) into (A12) yields the collision efficiency integral evaluated on the contact surface,

$$I_g^{(k)}(s_c) = \Gamma_g + \Lambda_g^{(0)} - \log f_g(\nu K^{2/5}),$$
 (3.17)

where

$$\Gamma_{g} = \lim_{\xi \to 0} \left[\int_{\xi}^{\infty} \frac{L_{0}(t) - M_{0}(t)}{(2+t)L_{0}(t)} dt + \log f_{g}(\xi) \right], \tag{3.18}$$

$$\Lambda_g^{(0)} = -\frac{1}{2R_g} \left[\int_1^\infty \left[M_{\xi}(\xi, q) f(q) - M_{\xi, 0}(\xi) \right] \frac{dq}{q} + \int_0^1 M_{\xi}(\xi, q) f(q) \frac{dq}{q} \right]. \tag{3.19}$$

Inserting this result into Eq. (2.25) yields the collision efficiency,

$$E_g^{(k)} = \left[e^{-\left(\Gamma_g + \Lambda_g^{(0)}\right)} f_g(\nu K^{2/5}) \right]^{-2}.$$
 (3.20)

C. Collision efficiency for uniaxial strain

The collision efficiency for permeable particles in uniaxial strain is given by Eq. (2.26). The analysis is closely analogous to that given above for gravity-induced collisions. The collision efficiency integral (2.26b) is evaluated on the contact surface by the procedure in Appendix A1. In this case, the required functions are

$$Q(s) = 1 - A(s), \quad P(s) = (A(s) - B(s))s^{-1}.$$
 (3.21)

From Eqs. (2.29c) and (2.31b), the lubrication forms are

$$Q_{\xi} = R_{st} \frac{\xi}{f(q)}, \quad P_{\xi} = \frac{1}{2} B'_{\xi}(\xi, q),$$
 (3.22)

where we define

$$B' = 1 - B. (3.23)$$

The corresponding functions, $1 - A_0$ and B_0 , for impermeable spheres are also required, and their lubrication forms are given by Eqs. (2.33c) and (2.34b). The required indefinite integral (A11) is

$$F_{st}(x) = \frac{1}{R_{st}} \int_{0}^{x} B'_{\xi,0}(t) \frac{dt}{2t} = \log f_{st}(x), \qquad (3.24)$$

and $f_{st}(x)$ is given by Eq. (A31) and $B'_{\xi,0}$ is defined by Eq. (3.23). Inserting this result with Eqs. (3.21) and (3.22) into (A12) yields the collision efficiency integral evaluated on the contact surface,

$$I_{st}^{(k)}(s_c) = \Gamma_{st} + \Lambda_{st}^{(0)} - \log f_{st}(\nu K^{2/5}),$$
 (3.25)

where

$$\Gamma_{st} = \lim_{\xi \to 0} \left[\int_{\xi}^{\infty} \frac{A_0(t) - B_0(t)}{(2+t)[1 - A_0(t)]} dt + \log f_{st}(\xi) \right]$$
(3.26)

and

$$\Lambda_{st}^{(0)} = \frac{1}{2R_{st}} \left[\int_{1}^{\infty} \left[B_{\xi}'(\xi, q) f(q) - B_{\xi, 0}'(\xi) \right] \frac{dq}{q} + \int_{0}^{1} B_{\xi}'(\xi, q) f(q) \frac{dq}{q} \right].$$
(3.27)

Inserting this result into Eq. (2.26) yields the collision efficiency,

$$E_{st}^{(k)} = \left[e^{-\left(\Gamma_{st} + \Lambda_{st}^{(0)}\right)} f_{st}(\nu K^{2/5}) \right]^{3}.$$
 (3.28)

D. Collision efficiency for shear flow

The contact values for two collision efficiency integrals are needed for the collision efficiency of particles in shear flow, according to Eq. (2.27). This includes the integral, $I_{st}(s_c)$, analyzed above, and $I_{sh}(s_c)$, given by Eq. (2.27b), evaluated below by the procedure in Appendix A1. For $I_{sh}(s_c)$, the required functions in Eq. (A1) are

$$Q(s) = 1 - A(s), \quad P(s) = \frac{1}{4}e^{-2I_{st}(s)}B(s)s.$$
 (3.29)

Here, the evaluation of the collision efficiency integral I_{st} is required away from the contact surface, which is facilitated by the procedure described in Appendix A3. The lubrication forms of Eq. (3.29) are obtained using Eqs. (A22) and (A23) and Eqs. (2.29c) and (2.31b),

$$Q_{\xi} = R_{st} \frac{\xi}{f(q)}, \quad P_{\xi} = \frac{1}{2} \left(e^{-(\Gamma_{st} + \Lambda_{st}(q))} f_{st}(\nu K^{2/5}) \right)^{2} B_{\xi}(\xi, q),$$

$$\xi = O(K^{2/5})$$
(3.30)

and

$$Q_{\xi,0} = R_{st} \, \xi \,, \quad P_{\xi,0} = \frac{1}{2} \left(e^{-\Gamma_{st}} f_{st}(\xi) \right)^2 B_{\xi,0}(\xi) \,, \quad K^{2/5} \ll \xi \ll 1 \,,$$
(3.31)

where Γ_{st} is given by Eq. (3.26) and $f_{st}(\xi)$ is given by Eq. (A31). The function $\Lambda_{st}(q)$ is generically defined by Eq. (A24) and is, in this case, given by

$$\Lambda_{st}(q) = \frac{1}{2R_{st}} \left[\int_{1}^{\infty} \left[B'_{\xi}(\xi, q') f(q') - B'_{\xi, 0}(\xi) \right] \frac{dq'}{q'} + \int_{q}^{1} B'_{\xi}(\xi, q') f(q') \frac{dq'}{q'} \right], \tag{3.32}$$

where B' is defined by Eq. (3.23). The additional indefinite integral (A11) needed for evaluating I_{sh} on the contact surface is

$$F_{sh}(\xi) = \frac{e^{-2\Gamma_{st}}}{2R_{st}} \int_{\xi}^{\xi} f_{st}^{2}(t) B_{\xi,0}(t) \frac{dt}{t} , \qquad (3.33)$$

where ξ_0 is an arbitrary constant.

Inserting the above elements into (A12) yields the collision efficiency integral evaluated on the contact surface,

$$I_{sh}^{(k)}(s_c) = \Gamma_{sh} + \Lambda_{sh}^{(0)} - F_{sh}(\nu K^{2/5}),$$
 (3.34)

where

$$\Gamma_{sh} = \lim_{\xi \to 0} \left[\int_{\xi}^{\infty} \frac{e^{-2I_{st,0}(t)} B_0(t)}{4[1 - A_0(t)]} (2 + t) dt + F_{sh}(\xi) \right]$$
(3.35)

and

$$\Lambda_{sh}^{(0)} = \frac{e^{-2\Gamma_{st}}}{2R_{st}} \left[\int_{1}^{\infty} \left[e^{-2\Lambda_{st}(q)} f_{st}^{2} (\nu K^{2/5}) B_{\xi}(\xi, q) f(q) - f_{st}^{2}(\xi) B_{\xi,0}(\xi) \right] \frac{dq}{q} + \int_{0}^{1} e^{-2\Lambda_{st}(q)} f_{st}^{2} (\nu K^{2/5}) B_{\xi}(\xi, q) f(q) \frac{dq}{q} \right].$$
(3.36)

Note that the value of ζ_0 used in Eq. (3.33) affects the value of Γ_{sh} but not the value of $I_{sh}^{(k)}(s_c)$.

Inserting this result together with Eqs. (3.25) into Eq. (2.27) yields

$$E_{sh}^{(k)} = \left[\left(e^{-\left(\Gamma_{st} + \Lambda_{st}^{(0)}\right)} f_{st}(\nu K^{2/5}) \right)^2 - \left(\Gamma_{sh} + \Lambda_{sh}^{(0)} - F_{sh}(\nu K^{2/5}) \right) \right]^{3/2},$$
(3.37)

where the quantity inside the square brackets is assumed to be positive, otherwise $E_{sh} = 0$. In shear flow, there exists a positive, size-ratio-dependent critical permeability, K_* , below which $E_{sh} = 0$. The critical permeability is a root of the equation

$$\left(e^{-\left(\Gamma_{st}+\Lambda_{st*}^{(0)}\right)}f_{st}\left(\nu K_{*}^{2/5}\right)\right)^{2}-\left(\Gamma_{sh}+\Lambda_{sh*}^{(0)}-F_{sh}\left(\nu K_{*}^{2/5}\right)\right)=0,$$
(3.38)

where $\Lambda_{st*}^{(0)}$ and $\Lambda_{sh*}^{(0)}$ denote evaluation at $K=K_*$. The existence of a critical permeability is analogous to the critical roughness below which particle contact does not occur in shear.²⁵

IV. COLLISION EFFICIENCY FORMULAS FOR ROUGH PARTICLES

The aggregation of particles with small-amplitude surface roughness $\delta \ll 1$ is considered in this section because of the qualitative similarity to the aggregation of permeable particles. Rough particles also have axisymmetric mobilities with non-zero contact values and can thus undergo aggregation in the absence of non-hydrodynamic interparticle forces. The $O(\delta)$ boundary layer that forms in the limit of small-amplitude roughness is analogous to the $O(K^{2/5})$ boundary layer formed with permeable particles in the weak-permeability limit (1.1).

The axisymmetric mobilities of particles with surface roughness have non-zero $O(\delta)$ contact values because the contact surface is, by definition, at a non-zero surface-to-surface separation, $\epsilon=\delta$; the contact values are obtained by inserting $\epsilon=\delta$ into the near-contact mobilities for impermeable particles Eqs. (2.33) and (2.34). For separations $\epsilon>\delta$, the mobilities of rough particles are identical to those for smooth, impermeable particles. $^{40-42}$

A. Collision efficiencies for rough particles

As shown in Appendix A2, the values of collision efficiency integrals at the contact surface, $s=2+\nu\delta$, for particles with small-amplitude surface roughness, δ , are directly obtained from the contact values of collision efficiency integrals for permeable particles by making the following substitution:

$$\Lambda^{(0)} \to F(\nu K^{2/5}) - F(\nu \delta). \tag{4.1}$$

This result is supported by Eq. (A25). By this procedure, the collision efficiencies for particles with small-amplitude surface roughness are derived below. A direct derivation of the formulas is presented in Appendix A2, and the parameters needed for evaluating the formulas are provided in Appendix B.

1. Brownian motion

By the procedure described above, using substitution (4.1), the collision efficiency for rough particles in Brownian motion is derived from Eq. (3.4) and is given by

$$E_B^{(\delta)} = \left[\Gamma_B - \frac{\nu}{2} E_1(A_\delta)\right]^{-1},\tag{4.2}$$

where Γ_B is given by Eq. (3.6), $E_1(x)$ is the exponential integral, and A_δ is the modified Hamaker parameter for rough particles,

$$A_{\delta} = \frac{\bar{A}_H}{6\delta} \ . \tag{4.3}$$

For $A_{\delta} \ll 1$, Eq. (4.2) reduces to

$$E_B^{(\delta)} = \left[\Gamma_{B,0} - \frac{\nu}{2}\log\nu\delta\right]^{-1}, \quad A_{\delta} \ll 1, \tag{4.4}$$

where $\Gamma_{B,0}$ is given by Eq. (3.11). The classical result (3.13) is recovered for $A_{\delta} \gg 1$; surface roughness has a negligible effect under these conditions.

2. Gravity sedimentation

The collision efficiency for rough particles undergoing sedimentation, derived from Eq. (3.20) by substitution (4.1), is

$$E_g^{(\delta)} = \left(e^{-\Gamma_g} f_g(\nu \delta)\right)^{-2},\tag{4.5}$$

where f_g is defined by Eq. (A30) and Γ_g is given by Eq. (3.18).

3. Uniaxial strain

The collision efficiency for rough particles in uniaxial strain, derived from Eq. (3.25) by substitution (4.1), is

$$E_{st}^{(\delta)} = \left(e^{-\Gamma_{st}} f_{st}(\nu \delta)\right)^3, \tag{4.6}$$

where f_{st} is defined by Eq. (A31) and Γ_{st} is given by Eq. (3.26).

4. Shear flow

By the same procedure, substituting Eq. (4.1) into Eq. (3.38), the collision efficiency of rough particles in shear flow is given by

$$E_{sh}^{(\delta)} = \left[\left(e^{-\Gamma_{st}} f_{st}(\nu \delta) \right)^2 - \left(\Gamma_{sh} - F_{sh}(\nu \delta) \right) \right]^{3/2}, \tag{4.7}$$

where f_{st} is given by Eq. (A31), Γ_{st} by Eq. (3.26), Γ_{sh} by (3.35), and F_{sh} by (3.33).

The size-ratio-dependent critical roughness, δ_* , below which $E_{sh}^{(\delta)}=0$, $E_{sh}^{(\delta)}=0$ is a root of the equation obtained by making the same substitution into Eq. (3.38), i.e.,

$$\left(e^{-\Gamma_{st}}f_{st}(\nu\delta_*)\right)^2 - \left(\Gamma_{sh} - F_{sh}(\nu\delta_*)\right) = 0. \tag{4.8}$$

B. Equivalent roughness

The qualitative similarity between the weakly permeable particles and the particles with small-amplitude surface roughness suggests the introduction of an equivalent roughness δ_{eq} defined by setting the corresponding collision efficiencies equal, $E^{(\delta_{eq})} = E^{(k)}$. Equating the collision efficiency for permeable and rough particles, by equating the contact values for the collision efficiency integrals (A12) and (A20), yields

$$F(\nu \delta_{eq}) - F(\nu K^{2/5}) + \Lambda^{(0)} = 0.$$
 (4.9)

This result suggests $\delta_{eq} \approx c_k K^{2/5}$, reflecting the respective boundary layer thicknesses for the two problems, where the coefficient c_k would be expected to depend on the aggregation mechanism and size ratio of the particles. Inserting this scaling and Eqs. (4.11), (A11), and (A14) into Eq. (4.9) yields an equation for the roughness coefficient, c_k

$$\int_{1}^{c_{k}} P_{\xi,0}(\xi) \frac{dq}{q} + \int_{1}^{\infty} \left[P_{\xi}(\xi,q) f(q) - P_{\xi,0}(\xi) \right] \frac{dq}{q} + \int_{0}^{1} P_{\xi}(\xi,q) f(q) \frac{dq}{q} = 0.$$
(4.10)

This relationship is not generally invertible except for constant P_{ξ} , and, under these conditions, c_k will be independent of size ratio. These conditions are met for particle aggregation under Brownian motion in the absence of the van der Waals attraction, according to Eq. (3.1b). Inserting Eqs. (3.1b) and (3.12) into relation (4.10) yields

$$\delta_{ea} = c_k K^{2/5}, \quad c_k = e^{-2\nu^{-1}\Lambda_{B,0}^{(0)}} \doteq 0.7224.$$
 (4.11)

The collision efficiency of the particles with permeability K under Brownian motion without the van der Waals attraction is thus rigorously related to the collision efficiency of particles with surface roughness δ_{eq} ; the result is independent of the size ratio. Defining the equivalent roughness by equating the collision rates in Brownian motion is mathematically equivalent to equating the contact time between the permeable and rough particles under the action of a constant force directed along their line-of-centers starting from an arbitrary separation outside of the lubrication region [cf. Ref. 39, Eqs. (4.24) and (4.26)].

Equation (4.11) holds for the constant P_{ξ} in Eq. (4.10). The nonconstant P_{ξ} arises because of the oblique trajectories that determine the collision efficiencies in sedimentation, uniaxial strain, and in shear flow. The transverse mobilities M and B are insensitive to permeability, thus $P_{\xi} \approx P_{\xi,0}^{\ 80}$ but the logarithmic behavior of $P_{\xi,0}$ at $\xi=0$, resulting from the lubrication forms of the transverse mobilities (2.34a), suggests that, while the scaling of Eq. (4.11) is expected to hold, the roughness coefficient, c_k , may be sensitive to the aggregation mechanism, size ratio, and the Hamaker constant (Brownian motion). However, the results presented below shows this sensitivity is very weak and support the robustness of Eq. (4.11) for all four aggregation mechanisms and parameter ranges considered herein.

V. NUMERICAL RESULTS AND DISCUSSION

In this section, the numerical results are presented for the collision efficiencies of permeable particles undergoing (i) Brownian motion, (ii) gravity sedimentation, (iii) uniaxial straining flow, and (iv) shear flow. In the latter case, the results are also presented for the critical permeability below which $E_{sh}\!=\!0$. The corresponding results for rough particles are also presented using the relationship (4.11). The procedure for evaluating the collision efficiencies is described in Appendix B.

Figures 1–5 reveal a very close quantitative agreement between the results for permeable and rough particles using an equivalent roughness defined by (4.11) for all four aggregation mechanisms over a wide range of parameter values; in most cases, the curves for permeable particles and particles with equivalent roughness are virtually indistinguishable.

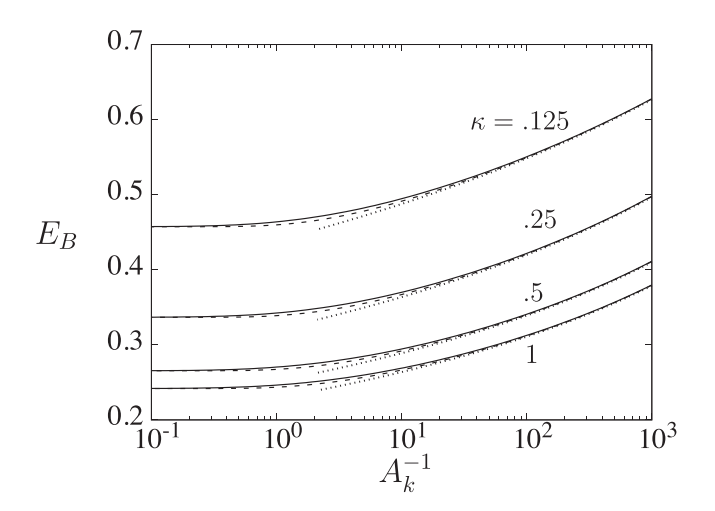


FIG. 1. Collision efficiencies for particles in Brownian motion, $\bar{A}_H = 10^{-4}$; permeable particles (3.4) (solid lines), rough particles (4.2) with $A_{\delta}^{-1} = c_k A_k^{-1}$ and c_k given by Eq. (4.11) (dashed lines), formula (3.10) (dotted lines); size ratios indicated.

To better understand why the equivalent roughness relationship (4.11) is applicable even for situations where the collision efficiency is determined by oblique, asymmetric trajectories, the influence of the transverse mobility was explored with and without incorporating the particle permeability. The dotted lines in Fig. 3 depict the results for permeable particles obtained using the axisymmetric lubrication formula (2.29c) for permeable particles with the transverse lubrication formula (2.34b) for the impermeable particles [i.e., in place of Eq. (2.31b)]. Although the particle permeability has no effect on the transverse pair mobility of equal size particles, it has a moderate O(1) effect on unequal size particles in close contact and qualitatively alters the near-contact motion for extreme size ratios. A comparison of the dotted and solid lines in Fig. 3, however, indicates that effect of permeability on the transverse mobility is barely perceptible even for $\kappa = .125$. This finding demonstrates the insensitivity of collision

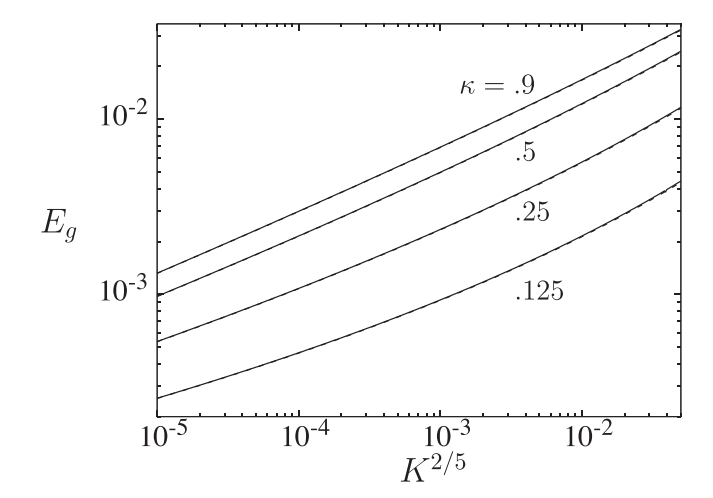


FIG. 2. Collision efficiencies for particles undergoing sedimentation, permeable particles (3.20) (solid lines), rough particles (4.5) with δ_{eq} given by Eq. (4.11) (dashed lines); size ratios indicated.

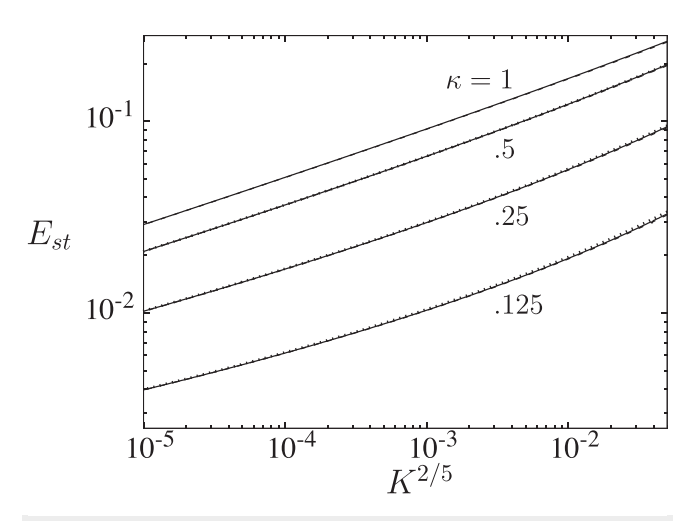


FIG. 3. Collision efficiencies for particles in uniaxial straining flow, permeable particles (3.28) (solid lines), rough particles (4.6) with $\delta_{\rm eq}$ given by Eq. (4.11) (dashed lines), permeable particles using impermeable transverse mobility function $B_{\xi,0}$ (dotted lines); size ratios indicated.

efficiencies to the transverse mobility and provides a plausible explanation for the robustness of the proposed equivalent roughness (4.11) for permeable particles.

Bäbler *et al.*⁵⁸ calculated the collision efficiencies for permeable particles in shear flow in complementary high-permeability regime, K = O(1). A reliable quantitative comparison to their results is not possible due to the disparity of the regimes considered. However, the results for the largest permeabilities presented in Fig. 4 appear to be in approximate agreement with the predictions of Bäbler *et al.*⁵⁸ for permeabilities in the smallest range they considered.

VI. CONCLUDING REMARKS

Permeability and roughness are analogous generic mechanisms that allow particle aggregation without the need for interparticle forces. Simplified asymptotic formulas for binary collision rates were derived

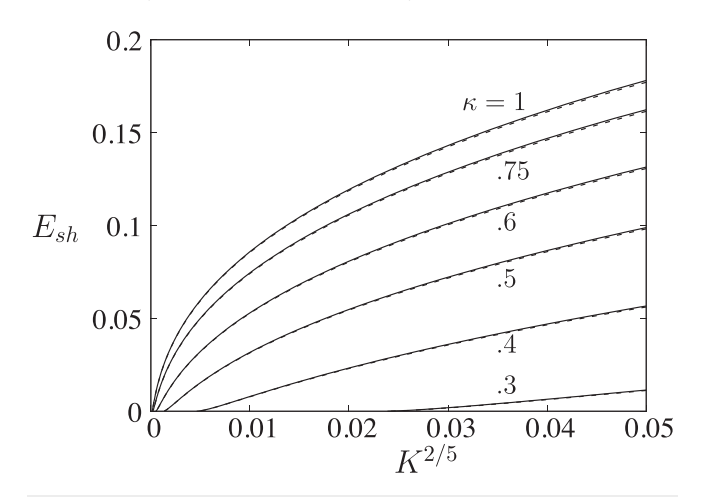


FIG. 4. Collision efficiencies for particles in shear flow, permeable (3.37) (solid lines), and rough particles (4.7) with δ_{eq} given by Eq. (4.11) (dashed lines); size ratios indicated.

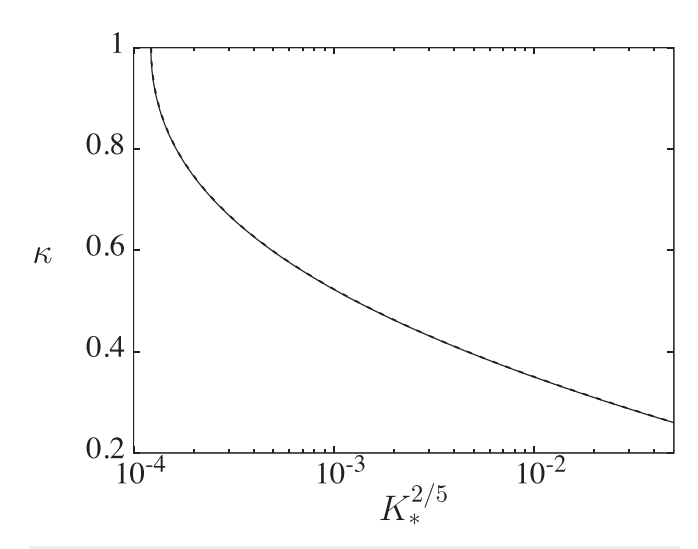


FIG. 5. Size ratio vs critical permeability (3.38) (solid lines) and critical roughness (4.8) with δ_{eq} given by Eq. (4.11) (dashed lines).

for weak permeability and small-amplitude roughness. A similar analysis could be developed for collision rates of drops with a low interfacial mobility. ⁸⁵

A quantitative relation between permeable and rough particles has been established through an equivalent roughness, allowing use of the simpler formulas for rough particles as approximations for the aggregation rate of permeable particles.

SUPPLEMENTARY MATERIAL

See the supplementary material for tabulated values of f(q) and g(q), and tables of coefficients for the transverse mobility functions M_{ξ} and B_{ξ} that appear in Eqs. (2.30)–(2.32). For further discussion of these quantities, see Refs. 39 and 80.

ACKNOWLEDGMENTS

The authors are grateful to Dr. A. Z. Zinchenko⁸⁶ for the use of his bispherical coordinate code for computing pair mobilities of hard spheres, and to Dr. D. J. Jeffrey⁸⁷ for the use of his program for resistance coefficients (https://www.uwo.ca/apmaths/faculty/jeffrey/) used here to obtain the axisymmetric resistances for hard spheres.

The authors acknowledge the support from the National Science Foundation CBET Grant No. 1603806. This work was financed in part by the Coordenação de Aperfeiçoamento de Pessoal de Nível Superior—Brasil (Capes)—Finance Code 001.

DATA AVAILABILITY

The data that support the findings of this study are available from the corresponding author upon reasonable request.

APPENDIX A: ASYMPTOTIC EVALUATION OF COLLISION EFFICIENCY INTEGRALS

In this Appendix, the collision efficiency integrals (2.24b)–(2.27b) are simplified for the case of weakly permeable particles and for particles with small-amplitude surface roughness.

1. Collision efficiency integrals for weakly permeable particles

The general approach to simplifying the evaluation of the integrals $I_x^{(k)}$ (x=B,g,st,sh) on the contact surface, $s_c=2$, for weakly permeable particles, $K\ll 1$, is to decompose the efficiency integrals into four parts and perform the near-contact integrations in the gap-width variable ξ ,

$$I^{(k)}(s_c) = \int_2^\infty \frac{P(s,q)}{Q(s,q)} ds = I^{(1)} + I^{(2)} + I^{(3)} + I^{(4)},$$
 (A1)

where the integrals are defined,

$$I^{(1)} = \int_{\xi_2}^{\infty} \frac{P_0(\xi)}{Q_0(\xi)} d\xi \,, \tag{A2}$$

$$I^{(2)} = \int_{\xi_1}^{\xi_2} \frac{P_{\xi,0}(\xi)}{Q_{\xi,0}(\xi)} d\xi, \qquad (A3)$$

$$I^{(3)} = \int_{\xi_1}^{\xi_2} \left[\frac{P_{\xi}(\xi, q)}{Q_{\xi}(\xi, q)} - \frac{P_{\xi, 0}(\xi)}{Q_{\xi, 0}(\xi)} \right] d\xi , \qquad (A4)$$

$$I^{(4)} = \int_0^{\xi_1} \frac{P_{\xi}(\xi, q)}{Q_{\xi}(\xi, q)} d\xi.$$
 (A5)

Here, ξ_1 and ξ_2 satisfy

$$K^{2/5} \ll \xi_2 \ll 1$$
, $\xi_1 = d_1 K^{2/5}$, (A6)

where d_1 is an arbitrary constant. Note that the variable q in integrals $I^{(3)}$ and $I^{(4)}$ is related to the integration variable, ξ , by Eq. (2.28).

The function Q in the above integrals is one of the axisymmetric mobility functions, G, L, or 1-A, and P is the nonsingular remainder of the collision efficiency integrand, i.e., combinations of the mobility functions as they appear in Eqs. (2.24b)-(2.27b), including the factors of s [and the exponential of the van der Waals potential in Eq. (2.24b)]. The functions P_0 and Q_0 correspond to the mobility functions for impermeable particles appropriate for $q\gg 1$. The functions P_ξ and Q_ξ are the near-contact, lubrication forms of P and Q, and $P_{\xi,0}$ and $Q_{\xi,0}$ are the near-contact forms of P_0 and P_0 0. The integrands for the collision efficiency integrals of impermeable spheres have non-integrable singularities, $Q_{\xi,0}\sim \xi$, at contact, leading to the divergence of the collision efficiency integrals (and vanishing of collision efficiencies) for impermeable spheres. Accordingly, $\xi_1 > 0$ is required for the integration limits of I_2 and I_3 above.

In the near-contact regime,

$$Q_{\xi} = R \frac{\xi}{f(a)},\tag{A7a}$$

$$Q_{\xi,0} = R\,\xi\,,\tag{A7b}$$

according to Eqs. (2.29) and (2.33), where R is the size-ratio-dependent contact resistance for the axisymmetric mobility function L or 1-A; for G, $R=\nu^{-1}$. Here, the function f(q) has asymptotic properties given by Eq. (2.30). The near-contact form P_{ξ} corresponds to the lubrication approximation of the integrands, obtained from Eqs. (2.29) and (2.31) [and Eq. (2.15) for integral (2.24b)].

Inserting Eq. (A7) into integrals (A3)–(A5) and taking account of the assumed orders of magnitude (A6) yield

$$I^{(2)} = \frac{1}{R} \int_{\xi_1}^{\xi_2} P_{\xi,0}(\xi) \frac{d\xi}{\xi} = F(\xi_2) - F(d_1 K^{2/5}), \qquad (A8)$$

$$I^{(3)} = \frac{1}{R} \int_{d_{z}=1}^{\infty} \left[P_{\xi}(\xi, q) f(q) - P_{\xi, 0}(\xi) \right] \frac{dq}{q} , \qquad (A9)$$

$$I^{(4)} = \frac{1}{R} \int_0^{d_1 \nu^{-1}} P_{\xi}(\xi, q) f(q) \frac{dq}{q} , \qquad (A10)$$

where *F* is the indefinite integral

$$F(x) = \frac{1}{R} \int_{-\infty}^{x} P_{\xi,0}(t) \frac{dt}{t} \,. \tag{A11}$$

Combining the above integrals and integral (A2), taking the limit $\xi_2 \to 0$, and arbitrary assigning $d_1 = \nu$, yields the desired result,

$$I^{(k)}(s_c) = \Gamma + \Lambda^{(0)} - F(\nu K^{2/5}), \qquad (A12)$$

where

$$\Gamma = \lim_{\xi \to 0} [I_0(\xi) + F(\xi)], \qquad (A13)$$

$$\Lambda^{(0)} = \frac{1}{R} \left[\int_{1}^{\infty} \left[P_{\xi}(\xi, q) f(q) - P_{\xi, 0}(\xi) \right] \frac{dq}{q} + \int_{0}^{1} P_{\xi}(\xi, q) f(q) \frac{dq}{q} \right]. \tag{A14}$$

Here, the quantity I_0 in Eq. (A13) is the collision efficiency integral for impermeable particles,

$$I_0(\xi) = \int_{\xi}^{\infty} \frac{P_0(t)}{Q_0(t)} dt$$
 (A15)

Recall that ξ and q in the integrand of Eq. (A14) are related by Eq. (2.28).

2. Collision efficiency integrals for particles with small-amplitude roughness

The corresponding analysis for the evaluation of the integrals integrals $I_x^{(\delta)}$ (x=B,g,st,sh) on the contact surface, $s_c=2+\nu\delta$, for small-amplitude surface roughness, $\delta\ll 1$, is similar to the foregoing analysis for weakly permeable particles but the situation is simpler because only impermeable sphere mobility functions are required. In this case, the integrals are decomposed into two parts,

$$I^{(\delta)}(s_c) = \int_{\nu\delta}^{\infty} \frac{P_0(s)}{Q_0(s)} ds = I^{(1)} + I^{(2)},$$
 (A16)

$$I^{(1)} = I_0(\xi_1) \,, \tag{A17}$$

$$I^{(2)} = \int_{\nu\delta}^{\xi_1} \frac{P_{\xi,0}(\xi)}{Q_{\xi,0}(\xi)} d\xi, \qquad (A18)$$

where I_0 is the collision efficiency integral for impermeable spheres (A15). Inserting Eq. (A7b) into the second integral yields

$$I^{(2)} = \frac{1}{R} \int_{\nu\delta}^{\xi_1} P_{\xi,0}(\xi) \frac{d\xi}{\xi} = F(\xi_1) - F(\nu\delta) , \qquad (A19)$$

where F(x) is the indefinite integral (A11). Here again, $\xi_1 > 0$ is required to avoid the singularity of $Q_{\xi,0}$ at contact. Rearranging these integrals and taking the limit $\xi_1 \to 0$ yield the desired result,

$$I^{(\delta)}(s_c) = \Gamma - F(\nu \delta), \qquad (A20)$$

where Γ is given by Eq. (A13).

Note that the contact value of the collision efficiency integrals for particles with surface roughness can be derived from the result for permeable particles by the substitution (4.1) in Eq. (A12). This result is justified below.

3. Evaluation of collision efficiency integral away from contact surface

The results for the evaluation of collision efficiency integrals off the contact surface are provided here. This is required for the evaluation of collision efficiencies in shear flow.

Outside of the near-contact region, the collision efficiency integral is given by the corresponding integral for impermeable particles (A15),

$$I(\xi) = I_0(\xi), \quad \xi = O(1).$$
 (A21)

Two distinct cases arise for the evaluation of collision efficiency integrals in the near-contact region,

$$I(q) = \Gamma + \Lambda(q) - F(\nu K^{2/5}), \quad \xi = O(K^{2/5}),$$
 (A22)

$$I(\xi) = \Gamma - F(\xi), \quad K^{2/5} \ll \xi \ll 1.$$
 (A23)

Here, F(x) is the integral defined by Eq. (A11), Γ is given by Eq. (A13), and $\Lambda(q)$ is the extension of Eq. (A14) for evaluation off of the contact surface,

$$\Lambda(q) = \frac{1}{R} \left[\int_{1}^{\infty} \left[P_{\xi}(\xi, q') f(q') - P_{\xi, 0}(\xi) \right] \frac{dq'}{q'} + \int_{q}^{1} P_{\xi}(\xi, q') f(q') \frac{dq'}{q'} \right]. \tag{A24}$$

Note that Eq. (A23) is actually equivalent to Eq. (A21) according to the definition (A13).

The result for evaluation on the contact surface, (A12), is recovered from Eq. (A22) for $q \rightarrow 0$ given that Eq. (A24) reduces to Eq. (A14). Equation (A22) reduces to Eq. (A23) for large q, given that

$$\lim_{q\to\infty} \Lambda(q) = F(\nu K^{2/5}) - F(\xi) \,. \tag{A25} \label{eq:A25}$$

Equation (A23) corresponds to the formula for rough spheres (A20) with roughness $\nu\delta=\xi$. This result justifies Eq. (4.1) because $q\to\infty$ corresponds to $K\to 0$ for $\xi>0$.

4. Two indefinite integrals

The two closely related indefinite integrals, F_g and F_{st} , defined by Eqs. (3.16) and (3.24), and needed, respectively, for

calculating the collision efficiencies in sedimentation and uniaxial straining flow are evaluated here. The derivation is similar to that presented in Davis [Ref. 27, Eq. (3.6)]. Both integrals have the form,

$$F(x) = \log f(x) \,, \tag{A26}$$

where

$$f(x) = \frac{x^{\alpha_1}}{(\log^2 x^{-1} + d_5 \log x^{-1} + d_4)^{\alpha_2}} \left(\frac{2 \log x^{-1} + d_5 - \Delta}{2 \log x^{-1} + d_5 + \Delta} \right)^{\alpha_3},$$

$$\alpha_1 = -\frac{d_3}{2R}, \quad \alpha_2 = \frac{d_3 d_5 - d_2}{4R},$$

$$\alpha_3 = \frac{2d_1 - d_2 d_5 + d_3 (d_5^2 - 2d_4)}{4R\Delta},$$
(A28)

and

$$\Delta = (d_5^2 - 4d_4)^{1/2} \,. \tag{A29}$$

The arbitrary constant associated with the indefinite integral, F(x), indicates that cf(x) can also be used, where c is an arbitrary constant; herein, we take c = 1.

For $F_g(x)$, defined by Eq. (3.16),

$$f_{g}(x) = f(x), \tag{A30}$$

with f(x) defined by (A27)–(A29), the coefficients given by $d_i = m_i$ (i = 1-5) in Eq. (2.34a), and $R = R_g$. For F_{st} , defined by Eq. (3.24),

$$f_{st}(x) = x^{1/(2R_{st})} f(x),$$
 (A31)

with f(x) as defined above, $d_i = b_i$ (i = 1-5) in Eq. (2.34b), and $R = R_{st}$.

APPENDIX B: NUMERICAL EVALUATION OF COLLISION EFFICIENCY FORMULAS

Here, we describe the parameters needed to evaluate the collision efficiency formulas derived in this paper and where to find them.

The size-ratio-dependent parameters R and Γ defined by Eqs. (A7) and (A13), respectively, depend on hard-sphere mobility functions G_0 , L_0 , M_0 , A_0 , and B_0 . The axisymmetric contact resistances, R, were evaluated using the resistance function code of Jeffrey⁸⁷ by the procedure described in Appendix D of Ref. 80. The parameters Γ were evaluated using a bispherical coordinate code provided by Zinchenko. ^{42,86} The values of these parameters for several size ratios are provided in Tables I and II.

The functions F(x) defined by Eq. (A11) require the size-ratio-dependent coefficients for the near-contact lubrication forms (2.34)

TABLE I. Contact forces for particles migrating in gravity ($\gamma = 1$) and in axisymmetric straining flow.

κ	1	0.9	0.75	0.6	0.5	0.4	0.3	0.25	0.125
R_g		0.7745	0.7500	0.6947	0.6357	0.5561	0.4538	0.3939	0.2175
R_{st}	4.077	4.059	3.947	3.691	3.415	3.034	2.530	2.226	1.285

TABLE II. Coefficients Γ for collision efficiencies of particles in Brownian motion, gravity sedimentation, straining flow, and shear flow. Here, Γ_{sh} is obtained with F_{sh} defined by integral (3.33) with $\xi_0 = \nu \times 10^{-5}$.

κ	1	0.9	0.75	0.6	0.5	0.4	0.3	0.25	0.125
$\Gamma_{B,0}$	1.528	1.526	1.513	1.482	1.449	1.403	1.341	1.301	1.156
Γ_g		-0.080	0.0042	0.202	0.413	0.674	0.889	0.916	0.410
Γ_{st}	-0.038	-0.045	-0.086	-0.186	-0.299	-0.446	-0.585	-0.618	-0.359
Γ_{sh}	0.6099	0.6148	0.6462	0.7228	0.8139	0.9551	1.173	1.324	1.917

of the standard hard-sphere mobility functions $M_{\xi,0}$ and $B_{\xi,0}$ which can be found in a text book.⁸⁸

Collision efficiency formulas for permeable particles also require the functions f(q) and g(q) that enter the lubrication forms (2.29) and (2.31) and the coefficients for M_{ξ} and B_{ξ} in Eqs. (2.31a) and (2.31b).^{39,80} For convenience, tabulated values of f(q) and g(q) and tables of coefficient values for the mobility functions are reproduced and provided as supplementary material. These parameters are needed for the functions $\Lambda^{(0)}$ defined by Eq. (A14).

REFERENCES

- ¹M. Elimelech, "Predicting collision efficiencies of colloidal particles in porous media," Water Res. **26**(1), 1–8 (1992).
- ²P. G. Saffman and J. S. Turner, "On the collision of drops in turbulent clouds," J. Fluid Mech. 1(1), 16–30 (1956).
- ³R. A. Shaw, "Particle-turbulence interactions in atmospheric clouds," Annu. Rev. Fluid Mech. 35(1), 183–227 (2003).
- ⁴G. A. Jackson, "Effect of coagulation on a model planktonic food web," Deep Sea Res., Part I 48(1), 95–123 (2001).
- ⁵J. Słomka and R. Stocker, "On the collision of rods in a quiescent fluid," Proc. Natl. Acad. Sci. 117(7), 3372–3374 (2020).
- ⁶J. Słomka and R. Stocker, "Bursts characterize coagulation of rods in a quiescent fluid," Phys. Rev. Lett. **124**, 258001 (2020).
- ⁷M. V. Smoluchowski, "Versuch einer mathematischen theorie der koagulationskinetik kolloider losungen," Z. Phys. Chem. **92U**, 129–168 (1918).
- ⁸N. Fuchs, "Über die stabilität und aufladung der aerosole," Z. Phys. **89**, 736–743 (1934).
- ⁹L. A. Spielman, "Viscous interactions in Brownian coagulation," J. Colloid Interface Sci. 33(4), 562–571 (1970).
- ¹⁰I. A. Valioulis and E. J. List, "Collision efficiencies of diffusing spherical-particles: Hydrodynamic, van der Waals and electrostatic forces," Adv. Colloid Interface Sci. 20, 1–20 (1984).
- ¹¹S. Kim and C. F. Zukoski, "A model of growth by heterocoagulation in seeded colloidal dispersions," J. Colloid Interface Sci. 139, 198–212 (1990).
- ¹²A. S. G. Curtis and L. M. Hocking, "Collision efficiency of equal spherical particles in a shear flow. The influence of London-van der Waals forces," Trans. Faraday Soc. 66, 1381–1390 (1970).
- ¹³P. A. Arp and S. G. Mason, "Orthokinetic collisions of hard spheres in simple shear flow," Can. J. Chem. 54(23), 3769–3774 (1976).
- ¹⁴G. R. Zeichner and W. R. Schowalter, "Use of trajectory analysis to study stability of colloidal dispersions in flow fields," AIChE J. 23(3), 243-254 (1977).
- 15 T. G. M. van de Ven and S. G. Mason, "The microrheology of colloidal dispersions VII. Orthokinetic doublet formation of spheres," Colloid Polym. Sci 255, 468–479 (1977).
- ¹⁶P. M. Adler, "Heterocoagulation in shear flow," J. Colloid Interface Sci. 83(1), 106–115 (1981).
- ¹⁷M. R. Greene, P. A. Hammer, and W. L. Olbricht, "The effect of hydrodynamic flow field on colloidal stability," J. Colloid Interface Sci. 167(2), 232–246 (1994).
- ¹⁸S. Melis, M. Verduyn, G. Storti, M. Morbidelli, and J. Baldyga, "Effect of fluid motion on the aggregation of small particles subject to interaction forces," AIChE J. 45(7), 1383–1393 (1999).

- ¹⁹M. Vanni and G. Baldi, "Coagulation efficiency of colloidal particles in shear flow," Adv. Colloid Interface Sci. 97(1), 151–177 (2002).
- 20E. J. Verway and J. T. Overbeek, Theory of Stability of Lyophobic Colloids (Elsevier, 1948).
- ²¹C. J. Lin, K. J. Lee, and N. F. Sather, "Slow motion of two spheres in a shear field," I. Fluid Mech. 43(1), 35–47 (1970).
- ²²G. K. Batchelor and J. T. Green, "The hydrodynamic interaction of two small freely-moving spheres in a linear flow field," J. Fluid Mech. 56(2), 375–400 (1972).
- 23G. K. Batchelor and J. T. Green, "The determination of the bulk stress in a suspension of spherical particles to order c²," J. Fluid Mech. 56(2), 401–427 (1972).
- ²⁴G. K. Batchelor, "Sedimentation in a dilute polydisperse system of interacting spheres. Part 1. General theory," J. Fluid Mech. 119, 379–408 (1982).
- 25P. A. Arp and S. G. Mason, "The kinetics of flowing dispersions: VIII. Doublets of rigid spheres (theoretical)," J. Colloid Interface Sci. 61(1), 21–43 (1977).
- ²⁶J. D. Klett and M. H. Davis, "Theoretical collision efficiencies of cloud droplets at small Reynolds numbers," J. Atmos. Sci. 30(1), 107–117 (1973).
- 27 R. H. Davis, "The rate of coagulation of a dilute polydisperse system of sedimenting spheres," J. Fluid Mech. 145, 179–199 (1984).
- ²⁸D. H. Melik and H. S. Fogler, "Gravity-induced flocculation," J. Colloid Interface Sci. 101(1), 72–83 (1984).
- ²⁹M. Han and D. F. Lawler, "The (relative) insignificance of G in flocculation," J. AWWA 84(10), 79–91 (1992).
- 30 X. Zhang and R. H. Davis, "The rate of collisions due to Brownian or gravitational motion of small drops," J. Fluid Mech. 230, 479–504 (1991).
- ³¹A. Z. Zinchenko, "Effect of hydrodynamic interactions between the particles on the rheological properties of dilute emulsions," J. Appl. Math. Mech. 48(2), 198–206 (1984).
- ³²H. Wang, A. Z. Zinchenko, and R. H. Davis, "The collision rate of small drops in linear flow fields," J. Fluid Mech. 265, 161–188 (1994).
- ³³M. Loewenberg and R. H. Davis, "Flotation rates of fine, spherical particles and droplets," Chem. Eng. Sci. 49(23), 3923–3941 (1994).
- ³⁴A. Z. Zinchenko and R. H. Davis, "Collision rates of spherical drops or particles in a shear flow at arbitrary Péclet numbers," Phys. Fluids 7(10), 2310–2327 (1995).
- 35V. Bal, "Stability characteristics of nanoparticles in a laminar linear shear flow in the presence of DLVO and non-DLVO forces," Langmuir 35, 11175–11187 (2019).
- 36 V. Bal, "Coagulation behavior of spherical particles embedded in laminar shear flow in presence of DLVO-and non-DLVO forces," J. Colloid Interface Sci. 564, 170–181 (2020).
- ³⁷A. Z. Zinchenko and R. H. Davis, "Gravity-induced coalescence of drops at arbitrary Péclet numbers," J. Fluid Mech. 280, 119–148 (1994).
- ³⁸J. A. Ramirez, A. Z. Zinchenko, M. Loewenberg, and R. H. Davis, "The flotation rates of fine spherical particles under Brownian and convective motion," Chem. Eng. Sci. 54, 149–157 (1999).
- ³⁹R. B. Reboucas and M. Loewenberg, "Near-contact approach of two permeable spheres," J. Fluid Mech. (to be published).
- ⁴⁰J. R. Smart and D. T. Leighton, "Measurement of the hydrodynamic surface roughness of noncolloidal spheres," Phys. Fluids A 1(1), 52–60 (1989).
- ⁴¹J. R. Smart, S. Beimfohr, and D. T. Leighton, "Measurement of the translational and rotational velocities of a noncolloidal sphere rolling down a smooth inclined place at low Reynolds number," Phys. Fluids A 5, 13–24 (1993).

- ⁴²M. S. Ingber and A. Z. Zinchenko, "Semi-analytic solution of the motion of two spheres in arbitrary shear flow," Int. J. Multiphase Flow 42, 152–163 (2012).
- ⁴³F. R. Da Cunha and E. J. Hinch, "Shear-induced dispersion in a dilute suspension of rough spheres," J. Fluid Mech. 309, 211–223 (1996).
- ⁴⁴I. Rampall, J. R. Smart, and D. T. Leighton, "The influence of surface roughness on the particle-pair distribution function of dilute suspensions of non-colloidal spheres in simple shear flow," J. Fluid Mech. 339, 1–24 (1997).
- 45 D. N. Sutherland, "A theoretical model of floc structure," J. Colloid Interface Sci. 25(3), 373–380 (1967).
- 46H. C. Brinkman, "A calculation of the viscous force exerted by a flowing fluid on a dense swarm of particles," Appl. Sci. Res. A 1, 27–34 (1949).
- ⁴⁷A. M. J. Davis, "Axisymmetric flow due to a porous sphere sedimenting towards a solid sphere or a solid wall: Application to scavanging of small particles," Phys. Fluids 13, 3126 (2001).
- ⁴⁸D. F. James and A. M. J. Davis, "Flow at the interface of a model fibrous porous medium," J. Fluid Mech. 426, 47–72 (2001).
- 49J. L. Auriault, "On the domain of validity of Brinkman's equation," Transp. Porous Media 79, 215–223 (2009).
- 50D. A. Nield and A. Bejan, Convection in Porous Media, 4th ed. (Springer, 2013).
- ⁵¹G. Neale, N. Epstein, and W. Nader, "Creeping flow relative to permeable spheres," Chem. Eng. Sci. 28, 1865–1874 (1973).
- ⁵²D. N. Sutherland and C. T. Tan, "Sedimentation of a porous sphere," Chem. Eng. Sci. 25(12), 1948–1950 (1970).
- ⁵³P. M. Adler, "Streamlines in and around porous particles," J. Colloid Interface Sci. 81(2), 531–535 (1981).
- 54S. Veerapaneni and M. R. Wiesner, "Hydrodynamics of fractal aggregates with radially varying permeability," J. Colloid Interface Sci. 177(1), 45–57 (1996).
- 55X. Li and B. E. Logan, "Collision frequencies of fractal aggregates with small particles by differential sedimentation," Environ. Sci. Technol. 31, 1229–1236 (1997).
- ⁵⁶X.-Y. Li and B. E. Logan, "Permeability of fractal aggregates," Water Res. 35(14), 3373–3380 (2001).
- ⁵⁷A. Thill, S. Moustier, J. Aziz, M. R. Wiesner, and J. Y. Bottero, "Flocs restructuring during aggregation: Experimental evidence and numerical simulation," J. Colloid Interface Sci. 243(1), 171–182 (2001).
- ⁵⁸M. U. Bäbler, J. Sefcik, M. Morbidelli, and J. Baldyga, "Hydrodynamic interactions and orthokinetic collisions of porous aggregates in the Stokes regime," Phys. Fluids 18, 013302 (2006).
- ⁵⁹R. B. Jones, "Hydrodynamic interactions of two permeable spheres i: The method of reflections." Phys. A **92**, 545–556 (1978).
- ⁶⁰M. U. Bäbler, "A collision efficiency model for flow-induced coagulation of fractal aggregates," AIChE J. 54(7), 1748–1760 (2008).
- 61S. L. Goren, "The hydrodynamic force resisting the approach of a sphere to a
- plane permeable wall," J. Colloid Interface Sci. 69, 78–85 (1979).

 62 A. Nir, "On the departure of a sphere from contact with a permeable membrane," J. Eng. Math. 15, 65–75 (1981).
- ⁶³L. Elasmi and F. Feuillebois, "Integral equation method for creeping flow around a solid body near a porous slab," Q. J. Mech. Appl. Math. 56, 163–185 (2003).
- ⁶⁴A. Debbech, L. Elasmi, and F. Feuillebois, "Green function for a Stokes flow near a porous slab," J. Appl. Math. Mech. 90, 920–928 (2010).

- ⁶⁵G. Z. Ramon, H. E. Huppert, J. R. Lister, and H. A. Stone, "On the hydrodynamic interaction between a particle and a permeable surface," Phys. Fluids 25, 073103 (2013).
- ⁶⁶S. Khabthani, A. Sellier, and F. Feuillebois, "Lubricating motion of a sphere towards a thin porous slab with Saffman slip condition," J. Fluid Mech. 867, 949–968 (2019).
- ⁶⁷R. H. Davis and A. Z. Zinchenko, "Particle collection by permeable drops," Phys. Rev. Fluids 3, 113601 (2018).
- ⁶⁸S. B. Chen, "Axisymmetric motion of multiple composite spheres: Solid core with permeable shell, under creeping flow conditions," Phys. Fluids 10, 1550 (1998).
- ⁶⁹S. B. Chen and A. Cai, "Hydrodynamic interactions and mean settling velocity of porous particles in a dilute suspension," J. Colloid Interface Sci. 217, 328–340 (1999).
- ⁷⁰ K. A. Kusters, J. G. Wijers, and D. Thoenes, "Aggregation kinetics of small particles in agitated vessels," Chem. Eng. Sci. 52(1), 107–121 (1997).
- ⁷¹H. Darcy, Les Fontaines Publiques de la Ville de Dijon (Dalmont, 1856).
- ⁷²Y. Cao, M. Gunzburger, F. Hua, and X. Wang, "Coupled Stokes-Darcy model with Beavers-Joseph interface boundary condition," Commun. Math. Sci. 8, 1–25 (2010).
- ⁷³G. S. Beavers and D. D. Joseph, "Boundary conditions at a naturally permeable wall," J. Fluid Mech. 30, 197–207 (1967).
- 74P. G. Saffman, "On the boundary condition at the surface of a porous medium," Stud. Appl. Math. 50, 93-101 (1971).
- ⁷⁵C. K. W. Tam, "The drag on a cloud of spherical particles in low Reynolds number flow," J. Fluid Mech. 38(3), 537–546 (1969).
- 76S. Childress, "Viscous flow past a random array of spheres," J. Chem. Phys. 56(6), 2527–2539 (1972).
- 77. D. Howells, "Drag due to the motion of a Newtonian fluid through a sparse random array of small fixed rigid objects," J. Fluid Mech. 64(3), 449–476 (1974).
- 78T. Lévy, "Fluid flow through an array of fixed particles," Int. J. Eng. Sci. 21(1), 11–23 (1983).
- ⁷⁹L. Durlofsky and J. F. Brady, "Analysis of the brinkman equation as a model for flow in porous media," Phys. fluids 30(11), 3329–3341 (1987).
- ⁸⁰R. B. Reboucas and M. Loewenberg, "Resistance and mobility functions for the near-contact of permeable particles," J. Fluid Mech. (submitted) (2021).
- ⁸¹J. Blawzdziewicz, E. Wajnryb, and M. Loewenberg, "Hydrodynamic interactions and collision efficiencies of spherical drops covered with an incompressible surfactant film," J. Fluid Mech. 395, 29–59 (1999).
- 82S. J. Glass and D. J. Green, "Permeability and infiltration of partially sintered ceramics," J. Am. Ceram. Soc. 82(10), 2745–2752 (2004).
- 83S. Chugunov, A. Kazak, M. Amro, C. Freese, and I. Akhatov, "Towards creation of ceramic-based low permeability reference standards," Materials 12(23), 2886 (2010)
- 84H. C. Hamaker, "The London-van der Waals attraction between spherical particles," Physica 4, 1058 (1937).
- 85 R. H. Davis, J. A. Schonberg, and J. M. Rallison, "The lubrication force between two viscous drops," Phys. Fluids A 1(1), 77–81 (1989).
- 86 A. Z. Zinchenko, personal communication (2018).
- 87 See D. J. Jeffrey, https://www.uwo.ca/apmaths/faculty/jeffrey/ for "Programs for Stokes resistance functions" (2021).
- ⁸⁸S. Kim and S. J. Karrila, Microhydrodynamics: Principles and Selected Applications (Dover Publications, Inc., 2005).